J. Membrane Biol. 93, 165-175 (1986)

The Journal of
Membrane Biology

The Carrier Reorientation Step in Erythrocyte Choline Transport: pH Effects and the Involvement of a Carrier Ionizing Group

R. Devés,† G. Reyes,† and R.M. Krupka‡

†Department of Physiology and Biophysics, University of Chile, Santiago 7, Chile and ‡Research Centre, Agriculture Canada, London, Ontario, N6A 5B7, Canada

Summary. Under zero-*trans* conditions, the facilitated transport of choline across the erythrocyte membrane is limited by the rate of reorientation of the free carrier; as a result the pH dependence of this step can be investigated, independent of other steps in transport. It is found that as the pH declines (between 8.0 and 6.0) the rate of inward movement of the free carrier rises and the rate of outward movements falls, so that the partition of the free carrier increasingly favors the inward-facing form. When the pH of the cell interior and of the medium are varied independently, the partition responds to the internal but not the external pH. The membrane potential, which varies somewhat as the pH is altered, has no effect on the carrier partition. The analysis of the results indicates that the carrier mobility is dependent on an ionizing group of pK_a 6.8, which is exposed on the cytoplasmic surface of the membrane in the inward-facing carrier; in the outward-facing carrier the ionizing group appears to be masked, in that its pK_a is shifted downward by more than one unit. The observations can be explained by assuming that an ionizing group is located in the wall of a gated channel connecting the substrate site with the cytoplasmic face of the cell membrane.

Key Words ionizing group · choline carrier · carrier reorientation · pH effects · erythrocytes · carrier mechanism

Introduction

There is evidence that carrier-mediated transport depends on a conformational change in the transport protein, as a result of which the substrate site moves across the membrane, or more precisely, becomes exposed on the opposite side. Though this process, referred to as carrier reorientation, plays a central role in transport, little is known about its molecular mechanism.

A difficulty in studying the process of carrier reorientation is that it is one of several consecutive steps that together bring about substrate translocation. As the carrier scheme in Fig. 1 shows, the substrate must first be bound to the carrier site exposed on one side of the membrane; the carrier complex then undergoes reorientation, and the substrate is released on the other side; finally, the free carrier reverses its orientation, regaining its original position. The problem therefore is to devise a methodology for observing effects on a single step, i.e., carrier movement in one direction.

It would be possible to isolate a single step in a complex mechanism if that step were rate limiting. Several lines of evidence have shown that in the choline transport system of erythrocytes, which depends on a mechanism corresponding to the kinetic scheme in Fig. 1 [4, 6, 10, 14], the slowest step in transport is the reorientation of the free carrier [3, 4, 6, 9, 13], with the rate constants in the scheme declining in the following order: k_{-1}, $k_{-2} \gg f_2$, $f_{-2} \gg f_1$, f_{-1}. The choline system would therefore lend itself to an investigation of the problem.

In the present study, we have addressed the following questions: Is the reorientation of the free carrier sensitive to pH? If so, do inward and outward movement of the carrier have the same pH dependence? Also, is the system affected by both the internal and external pH?

We find that carrier reorientation is indeed sensitive to pH, but surprisingly, that inward and outward movement have an opposite pH dependence, the rate of the former rising and of the latter falling at declining pH values; also unexpected is that the system is sensitive to the pH on only one side of the membrane, that inside the cell. We show that the behavior can be explained by a single ionizing group exposed on the inner surface of the membrane, which affects the mobility of the free carrier: the outer carrier form becomes more mobile when this group is protonated, while the inner carrier becomes less mobile. Further, we suggest that the ionizing group is located in a gated channel connecting the substrate site with the inner surface of the

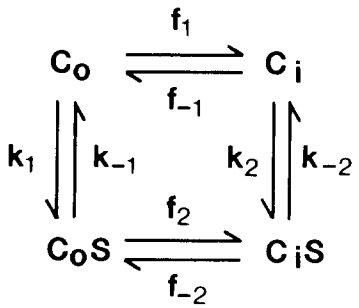

Fig. 1. Kinetic scheme for the carrier model. The conformation of the carrier alternates between inward-facing and outward-facing forms, C_o and C_i. Substrate molecules in the external or internal solutions, S_o and S_i, respectively, add to these two forms of the carrier; the corresponding substrate dissociation constants are $K_{So} = k_{-1}/k_1$ and $K_{Si} = k_{-2}/k_2$

membrane, and that it may function by alternately stabilizing the open and closed states of the channel.

Materials and Methods

1. Preparation of Cells

Human blood was obtained fresh from donors, using heparin as an anticoagulant. Cells (5% suspension) were washed free of endogenous choline by incubation at 37°C for two periods of three hours with 5 mM sodium phosphate buffer, pH 6.8, containing 154 mM NaCl.

2. Exit Assay

Loading with Radioactive Choline

Choline-free cells (50% hematocrit) were incubated overnight (approximately 14 hr) at 37°C in 5 mM sodium phosphate buffer, pH 6.8, containing [^{14}C]-choline chloride and 0.02% chloramphenicol. The concentration of choline was varied, depending on the type of experiment.

pH Equilibrium

Following the loading period, the cells were washed four or five times with a solution containing 35 mM sodium phosphate, 5 mM sodium bicarbonate, and enough NaCl for isotonicity, at the desired pH. After four washes a stable pH was achieved. Unless otherwise stated this buffer was used in all transport assays.

Transport Rate Measurement

Aliquots of loaded cells were added (10% hematocrit) to buffer at the desired pH, either in the presence or absence of unlabeled choline at a saturating concentration. The temperature was 37°C. Samples (0.9 ml) were withdrawn at intervals out to 10 min and rapidly centrifuged in tubes containing 0.3 ml dibutyl phthalate; the radioactivity in the supernatant solution (0.7 ml) was determined by scintillation counting. Rates were calculated from the initial linear relationship between counts and time.

3. Entry Assay

Transport Rate Measurement

Entry rates were measured by adding cells (10% hematocrit), previously washed at the desired pH, to a solution containing radioactive choline. Samples (0.8 ml) were withdrawn at intervals and added to tubes containing 0.5 ml of dibutyl phthalate. Upon centrifugation, the cells sedimented below the organic layer, which separated them from the aqueous radioactive solution above. The aqueous layer was removed by aspiration, and the walls of the tubes were thoroughly washed to eliminate contaminating radioactivity. Then, after removal of the dibutyl phthalate, the cells were precipitated by adding 0.3 ml of water and 0.3 ml 10% trichloroacetic acid. After centrifugation, the radioactivity in 0.5 ml of the supernatant was counted.

Loading the Cells with Unlabeled Choline

Some uptake experiments involve measuring the entry of radioactive choline into cells previously loaded with unlabeled choline. The loading was performed by incubating cells (20% hematocrit) with 200 μM choline in phosphate buffer (5 mM) for a period of 18 hr at 37°C. In order to estimate the final concentration of choline in the cells, another suspension was incubated with 200 μM radioactive choline over the same period of time, and the radioactivity in the cells was determined after precipitation with trichloroacetic acid.

4. Flux Ratio as a Function of Internal and External pH

Cells were incubated in buffered solutions at a particular pH for 1.5 hr at 37°C. They were then packed and suspended in the same buffer, containing 0.4 mM 4,4′-diisothiocyanostilbene-2,2′-disulfonic acid (DIDS) and 4 μM ^{14}C-choline. After overnight incubation, the choline-loaded cells were washed in cold buffer containing DIDS, in order to remove choline in the medium, and were packed by centrifugation. Exit rates were determined by the methods described above, with DIDS in the exit medium. By inhibiting the anion exchange system of the cells, specifically the exchange of bicarbonate and chloride ions, DIDS prevents the pH from equilibrating across the membrane [1]. The buffers used in these experiments were made up as follows: 143 mM NaCl containing either 25 mM PIPES (pH 6.8), 25 mM MES (pH 6.0), or 25 mM Tricine (pH 8.0).

5. Cell Volume as a Function of pH

Cells were washed in solutions at pH 6.8 and centrifuged at 1500 $\times$ g for 10 min. Aliquots of the packed cells (120 μl) were added to 20 ml of buffer (35 mM sodium phosphate and 5 mM $NaHCO_3$ in 120 mM NaCl) at a particular pH and allowed to equilibrate at 37°C. The suspension (9 ml) was centrifuged in a capillary tube having an enlarged upper section; the cells then became packed

Table 1. Cell volume as a function of pH

pH	Relative cell volume	Relative aqueous volume[a]
6.0	1.16 ± 0.028	1.21 ± 0.032
6.8	1.00 ± 0.024	1.00 ± 0.028
8.0	0.97 ± 0.050	0.92 ± 0.058

[a] Relative aqueous volumes were calculated by assuming that the aqueous volume is 70% of the total cell volume at pH 6.8.

in the capillary, and the height of the column of cells was measured with the aid of a cathetometer, with the capillary tube in a water bath at 37°C. The capillaries were calibrated with weighed amounts of pure water. The relative cell volumes at pH 6.0, 6.8 and 8.0 are recorded in Table 1.

6. The Partition of Chloride Ion

A one-ml aliquot of a 10% suspension of cells in isotonic buffer at 37°C was added to a microcentrifuge tube containing a small volume (up to 10 μl) of a solution of ^3H_2O (2 μCi), $Na^{36}Cl$ (0.03 μCi) or hydroxymethyl ^{14}C inulin (0.15 μCi). Each condition was run in triplicate. The suspensions were mixed and incubated for 15 min at 37°C. Dibutyl phthalate (0.3 ml) was added to each tube and the suspensions were centrifuged. Samples of the supernatant (100 μl) were taken for radioactivity determination, after which the supernatant and the organic layer were removed. The cells were suspended in 0.5-ml buffer, and 0.5 ml of 5% trichloroacetic acid was added; after centrifugation, a 0.7-ml sample was taken for counting.

The fraction of extracellular water in packed cells was determined from the results with inulin, which does not enter the cells. After correcting for this volume, the relative concentration of chloride ion in the cells and the medium was calculated from the ratio of counts in $^{36}Cl^-$ and tritiated water in each compartment.

Results

1. pH Dependence of the Maximum Rates of Entry and Exit

Rates of zero-*trans* entry and zero-*trans* exit were determined at varying substrate concentrations, at pH 6.0, 6.8 and 8.0. Double-reciprocal plots ($1/v$ against $1/[S]$) of the results at pH 6.0 and 8.0 are shown in Fig. 2. The maximum rates of exit and entry are found to be oppositely affected by pH, exit rates increasing as the hydrogen ion concentration is raised and entry rates decreasing. The average values of the relative maximum velocities measured in two experiments, as a function of pH, are shown in Table 2. The maximum rates were estimated by two different analytical methods [15]: (i) an $[S]/v$ against $[S]$ plot, and (ii) the direct linear plot. The rates in the Table have been corrected to take into account the effect of pH on the cell volume (Table 1); they are expressed as relative values, the maximum rate at pH 6.8 being taken as unity.

In the detailed analysis of the results, reliance will be placed mainly on measurements of maximum rates of entry rather than exit. The latter cannot be determined with precision because of the difficulty of loading the cells with saturating substrate concentrations, particularly at pH 6.0 where the substrate affinity is very low.

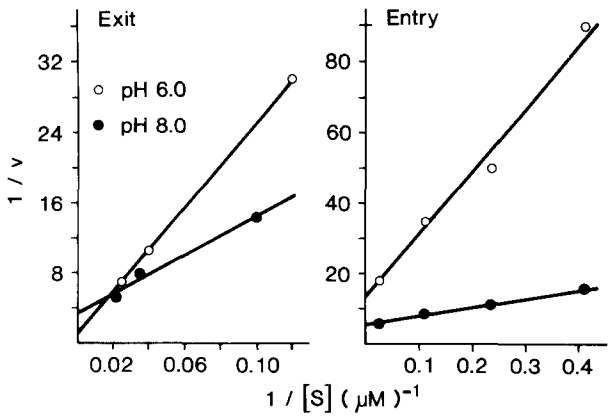

Fig. 2. Lineweaver-Burk plots for choline entry and exit at pH 6.0 and 8.0, in zero-*trans* experiments. The maximum rates calculated from the intercepts on the ordinate are (μmol per min per liter of cells): (i) Entry: pH 6.0, $\overline{V}_{So} = 0.078 \pm 0.024$; pH 8.0, $\overline{V}_{So} = 0.179 \pm 0.011$. (ii) Exit: pH 6.0, $\overline{V}_{Si} = 0.80 \pm 0.164$; pH 8.0, $\overline{V}_{Si} = 0.28 \pm 0.091$

Table 2. Relative maximum velocities for choline entry and exit as a function of pH[a]

Experiment		pH 6.0	pH 6.8	pH 8.0
ENTRY ($\overline{V}_{So}$)				
1	a	0.58 ± 0.033	1.0 ± 0.034	1.24 ± 0.043
	b	0.76	1.0	1.24
2	a	0.63 ± 0.035	1.0 ± 0.046	1.22 ± 0.028
	b	0.61	1.0	1.20
Average	a	0.60	1.0	1.23
	b	0.69	1.0	1.22
EXIT	($\overline{V}_{Si}$)			
1	a	3.71 ± 0.941	1.0 ± 0.176	0.49 ± 0.058
	b	4.59	1.0	0.47
2	a	2.90 ± 0.390	1.0 ± 0.149	1.12 ± 0.304
	b	2.63	1.0	1.27
Average	a	3.30	1.0	0.85
	b	3.61	1.0	0.87

[a] The results obtained in two experiments, involving different cell samples (1 and 2), and their average, are recorded. Rates were estimated by two different analytical methods, a) an $[S]/v$ *vs.* $[S]$ plot, and b) the direct linear plot [15]. The rates are expressed in relation to those at pH 6.8, which are set at unity.

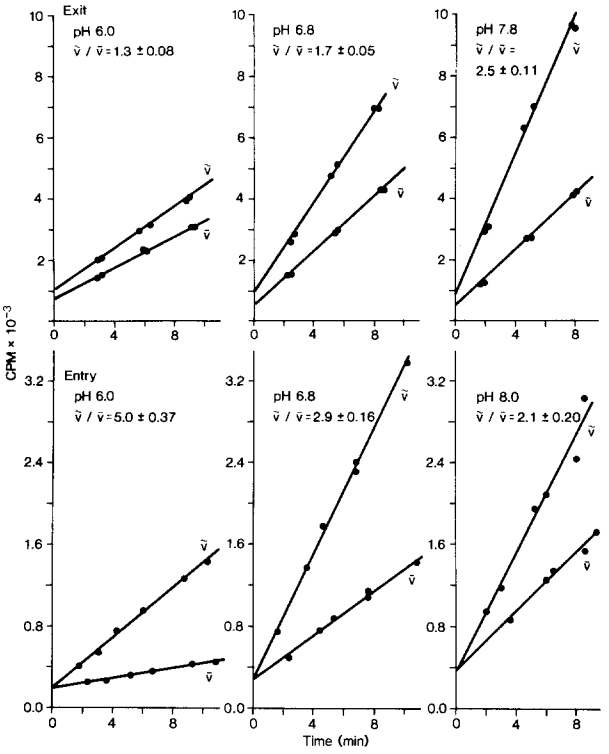

Fig. 3. Entry and exit of a low concentration of ^{14}C-choline at different pH values. Exit was measured either into pure buffer ($\bar{v}$) or into a medium containing 740 μM unlabeled choline ($\tilde{v}$). The initial choline concentration inside was 1.8 μM. Entry was measured into cells depleted of endogenous choline ($\bar{v}$) or into cells containing 87 μM unlabeled choline ($\tilde{v}$). The initial choline concentration outside was 0.78 μM. In each experiment the ratio of these two rates, $\tilde{v}/\bar{v}$, is recorded

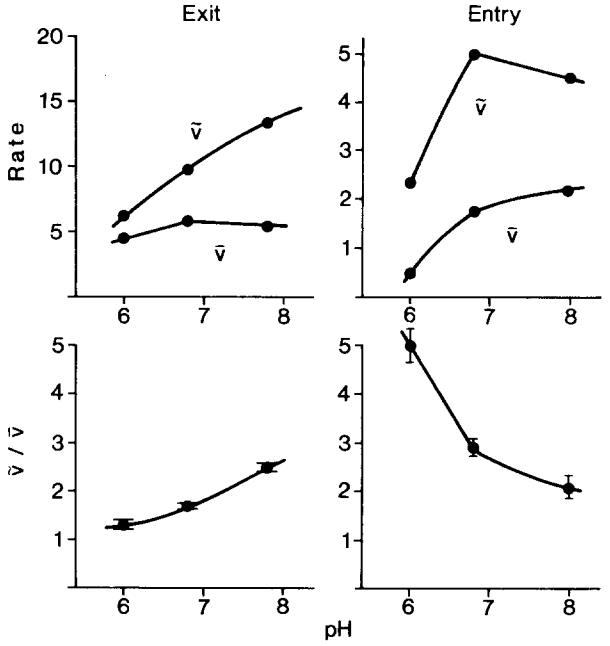

Fig. 4. Effect of pH on the flux ratio for choline entry and exit. The upper panel shows entry and exit rates under zero-*trans* ($\bar{v}$) and infinite-*trans* ($\tilde{v}$) conditions, as a function of pH. The rates, in units of μmol min^{-1} × liter cells^{-1} were calculated from the data in Fig. 3 and corrected to take into account the effect of pH on the cell volume (Table 1). The reference volume of the cells is that at pH 6.8. The lower panel shows the pH dependence of the calculated flux ratio ($\tilde{v}/\bar{v}$), the ratio of the infinite-*trans* and zero-*trans* rates

2. pH Dependence of the Flux Ratios for Entry and Exit

In the choline system, the distribution of the carrier between its inward- and outward-facing forms, given by the ratio of rate constants f_1/f_{-1}, may be determined most directly from the flux ratio, i.e., the ratio of the flux of a low concentration of radioactive choline into a medium containing a saturating concentration of unlabeled choline ($\tilde{v}$) and into a medium free of chloline ($\bar{v}$). Figure 3 shows such rate determinations for entry and exit at pH 6.0, 6.8 and 8.0. Exit rates are measured either into pure buffer ($\bar{v}$) or into a high concentration of unlabeled choline ($\tilde{v}$). Conversely, entry rates are measured into cells depleted of endogenous choline ($\bar{v}$) or into cells loaded with unlabeled choline ($\tilde{v}$). The calculated rates, as well as their ratio (the flux ratio, $\tilde{v}/\bar{v}$) are plotted against pH in Fig. 4. It is seen that while the flux ratio for exit increases with rising pH, the flux ratio for entry decreases.

The flux ratios for exit determined in six different experiments are in good agreement (Table 3). On the other hand, the ratios for entry, determined in eight experiments, are variable, though the trend in every experiment is the same, with the ratio increasing markedly as the pH declines (Table 4). There are two reasons for this variability: a) the difficulty already mentioned of loading the cells with sufficiently high concentrations of unlabeled choline, which would tend to lower the flux ratio, particularly at pH 6.0 where the internal substrate affinity is low; and b) the possibility that in some cell samples the external concentration of labeled choline could be too high relative to the external half-saturation constant, which would raise the ratio, principally at pH 8.0 and 6.8.

In spite of this problem, there is good agreement, as may be seen in Table 4, between the observed values for the entry flux ratios and the values predicted from the experimental ratios for exit, according to Eq. (10).

Table 3. Flux ratios for choline exit, $(\vec{v}/v)_{Si\to 0}$, at different pH values[a]

	pH	Flux ratio						
		1	2	3	4	5	6	Average
	6.0	1.33	1.22	1.30	1.34	1.30	1.11	1.27 ± 0.080
	6.8	1.66	1.80	1.84	2.19	1.74	1.87	1.85 ± 0.167
	7.8	2.45	2.65	—	—	—	—	2.55 ± 0.100
	8.0	—	—	2.86	3.23	2.50	2.54	2.78 ± 0.294
Substrate concentration[b]								
$[S_i^*]$ μM		5.1	3.5	2.4	2.6	1.8	2.9	
$[S_o]$ μM		920	740	740	740	740	740	

[a] Flux ratios were determined in experiments with six different cell samples (1–6).
[b] The concentration of radioactive choline inside the cell at the beginning of the experiment ($[S_i^*]$) is given, as well as the concentration of unlabeled choline outside ($[S_o]$) used in the measurement of the infinite-*trans* rate ($\vec{v}$).

Table 4. Flux ratios for choline entry, $(\vec{v}/v)_{So\to 0}$, at different pH values[a]

	pH	Flux ratio									
		1	2	3	4	5	6	7	8	Average	Predicted
	6.0	5.72	4.75	—	2.41	4.98	5.57	3.03	3.07	4.21 ± 1.25	4.70 ± 1.10
	6.8	3.32	1.87	1.81	2.0	2.87	2.87	1.81	2.09	2.33 ± 0.56	2.18 ± 0.23
	8.0	2.26	1.30	1.30	1.54	2.06	2.41	1.02	1.41	1.66 ± 0.48	1.56 ± 0.09
Substrate concentration[b]											
$[S_i]$ μM		107	57	54	48	87	123	58	58		
$[S_o^*]$ μM		0.65	0.36	0.36	0.69	0.78	0.61	0.62	0.31		

[a] Flux ratios were determined in experiments with eight different cell samples (1–8). The average of the experimental values at each pH is compared with the value predicted on the basis of the experimental flux ratio for exit (Table 3), according to Eq. (10).
[b] The concentration of radioactive choline outside ($[S_o^*]$) at the beginning of the experiment is given, as well as the concentration of unlabeled choline inside ($[S_i]$) used in the measurement of the infinite-*trans* rate ($\vec{v}$).

3. Effect of Internal and External pH on the Flux Ratio

In experiments in which the internal and external pH were altered independently, with the use of an inhibitor of the anion exchange system (DIDS), the flux ratio for exit was found to vary in response to the internal pH, but was insensitive to the pH in the external medium (Table 5).

Table 5. Dependence of the flux ratio for exit on the external and internal pH (pH_o and pH_i, respectively)[a]

pH_o	pH_i	$(v/v)_{Si-0}$
5.96	6.7	1.56 ± 0.08
6.72	6.7	1.88 ± 0.11
7.99	6.7	1.61 ± 0.15
6.73	6.0	1.42 ± 0.10
6.74	6.8	1.67 ± 0.10
6.79	7.9	2.26 ± 0.13

[a] The cells were treated with DIDS, an inhibitor of the anion exchanger, to prevent equilibration of hydrogen ions across the cell membrane (*see* Materials and Methods, section 4).

4. Dependence of the Flux Ratio on the Membrane Potential

Varying the pH of the red cell in the range 6 to 8 induces a small change in membrane potential, from 6.2 to −9.1 mV, as reported by Gunn et al. [8]. It was therefore necessary to investigate the relationship between the membrane potential alone and the carrier partition. With this aim, the flux ratio was measured in a solution in which 119 mM Cl^- had

Table 6. The flux ratio for exit at different membrane potentials (V)[a]

pH_o[b]	pH_i[b]	rCl	ΔV (mV)	$(\bar{v}/v)_{Si\to 0}$	f_1/f_{-1}
6.6	7.11	3.21 ± 0.065 (2)	31.1	2.21 ± 0.08 (2)	0.83 ± 0.06
6.8	6.84	1.09 ± 0.01 (2)	2.3	1.85 ± 0.167 (6)	1.18 ± 0.24

[a] rCl is the equilibrium distribution of chloride ion inside and outside the cell, $[Cl]_i/[Cl]_o$. The partition constant for the free carrier across the membrane, f_1/f_{-1}, which is equal to $[C_i]/[C_o]$, was calculated from the flux ratio for exit, $(\bar{v}/v)_{Si\to 0}$, using Eq. (8). The number of separate experiments in each determination is given by the number in brackets.

[b] The pH of the medium, pH_o, was measured directly in the cell suspension; the pH inside the cells, pH_i, was calculated from this pH together with the value of the partition of chloride ions, rCl, measured under the same conditions $[H^+]_o/[H^+]_i = r\text{Cl} = [Cl^-]_i/[Cl^-]_o$.

been replaced by 79 mM tartrate, at an external pH of 6.6 [7]. In this solution the membrane potential estimated from the chloride distribution ratio was 31.1 mV. The results, in Table 6, indicate that the membrane potential has little or no effect on the flux ratio (*see* Discussion, section 4).

Discussion

1. Effect of pH on the Mobility of the Free Carrier

As was noted in the Introduction, the maximum rate of transport into a choline-free solution is limited by the rate of reorientation of the free carrier. This conclusion is supported by evidence from three different types of experiments, namely accelerated exchange [5, 9, 13], noncompetitive inhibition by a nontransported substrate analog present in the *trans* compartment [5], and inactivation of the system by N-ethylmaleimide in the presence of substrates and substrate analogs [4, 6, 14]. Taken together, the observations show that (i) dissociation of the substrate is rapid compared with the reorientation of the free carrier or the carrier-substrate complex, and (ii) reorientation of the complex is rapid compared with that of the free carrier; i.e., in terms of the carrier scheme in Fig. 1, $k_{-1}, k_{-2} \gg f_2, f_{-2} \gg f_1, f_{-1}$.

Substitution of these inequalities into general expressions for the maximum rates of zero-*trans* entry ($\overline{V}_{So}$) and zero-*trans* exit $\overline{V}_{Si}$) yields the following simple equations [2, 11]:

$$\overline{V}_{So} = \frac{k_{-2}f_{-1}f_2[C_t]}{k_{-2}(f_{-1}+f_2)+f_{-1}(f_2+f_{-2})} \simeq f_{-1}[C_t] \quad (1)$$

$$\overline{V}_{Si} = \frac{k_{-1}f_1f_{-2}[C_t]}{k_{-1}(f_1+f_{-2})+f_1(f_2+f_{-2})} \simeq f_1[C_t]. \quad (2)$$

The observation that at increasing hydrogen ion concentration $\overline{V}_{So}$ decreases and $\overline{V}_{Si}$ increases therefore implies that f_{-1} decreases and f_1 increases. This in turn implies that the inner carrier form is more and more favored as the pH declines, for at equilibrium the partition of the carrier between inner and outer forms (C_i and C_o in Fig. 1) is given by:

$$\frac{[C_i]}{[C_o]} = \frac{f_1}{f_{-1}}. \quad (3)$$

2. Effect of pH on the Partition of the Free Carrier

In order to test the conclusion reached above, we have measured f_1/f_{-1} more directly. A kinetic analysis of the carrier model shows that in the choline system f_1/f_{-1} can be found from the flux ratio, i.e., from a comparison of zero-*trans* and infinite-*trans* transport rates [9]; specifically, the ratio is found from measurements of the flux of a low concentration of radioactive choline either into a medium containing a saturating concentration of unlabeled choline or into pure buffer. To explain the method, we may note first that the rate of unidirectional efflux at a fixed choline concentration is proportional to the concentration of the carrier in the inner form (C_i):

$$v = f_{-2}[CS_i] = f_{-2}[C_i][S_i]/K_{Si}. \quad (4)$$

Not all the carrier is in the form of C_i, of course; some also exists as the free outward-facing form C_o, but there is no significant concentration of the substrate complex, a condition ensured by the use of a very low concentration of the radioactive substrate in the experiment. The total carrier concen-

tration $[C_t]$ is therefore the sum of the concentrations of the inner and outer forms of the free carrier, which are in equilibrium:

$$[C_t] = [C_i] + [C_o]. \tag{5}$$

By contrast, when the cells are placed in a solution of unlabeled choline at a saturating concentration, practically all the carrier accumulates under steady-state conditions as the free inward-facing form. The reason is as follows: the substrate complex moves inward and is quickly unloaded, releasing the free carrier; but the free carrier is slow to move back across the membrane and therefore accumulates. Under these conditions, where $[C_i] \simeq [C_t]$, the rate of exit of radioactive substrate increases, according to Eq. (4), and becomes equal to

$$\vec{v} = f_{-2}[C_t][S_i]/K_{Si}. \tag{6}$$

The ratio of rates in the presence ($\vec{v}$) and absence ($\bar{v}$) of unlabeled choline outside may therefore be found from Eqs. (4) and (6):

$$\left(\frac{\vec{v}}{\bar{v}}\right)_{Si\to 0} = \frac{[C_t]}{[C_i]}. \tag{7}$$

Introducing Eq. (5) into Eq. (7) yields

$$\left(\frac{\vec{v}}{\bar{v}}\right)_{Si\to 0} = \frac{[C_i] + [C_o]}{[C_i]} = 1 + \frac{[C_o]}{[C_i]} = 1 + \frac{f_{-1}}{f_1}. \tag{8}$$

A general derivation of this equation was presented earlier [2]. Equation (8) indicates that the rate increase on addition of external substrate depends on the partition of the free carrier in the undisturbed system: if the carrier is predominantly inward-facing ($[C_i] \simeq [C_t]$), external substrate should have little or no effect, but if it is predominantly outward-facing ($[C_i] \ll [C_t]$) there should be a large acceleration of the rate.

Through a similar line of reasoning, the flux ratio for transport in the reverse direction, that is, for entry, is found to be:

$$\left(\frac{\vec{v}}{\bar{v}}\right)_{So\to 0} = 1 + \frac{[C_i]}{[C_o]} = 1 + \frac{f_1}{f_{-1}}. \tag{9}$$

According to these equations, the effect of pH on the flux ratios for exit and entry should be predictable from the effect of pH on the maximum zero-*trans* rates. If at declining pH values the maximum rate of exit, and therefore f_1, increases and the maximum rate of entry, and therefore f_{-1}, decreases (Table 1), then the flux ratio for exit should decrease (Eq. 8), and the flux ratio for entry should increase (Eq. 9). Moreover, the carrier model predicts a definite relationship between the flux ratios for entry and exit, based on Eqs. (8) and (9); the relationship takes the following form:

$$\left\{\left(\frac{\vec{v}}{\bar{v}}\right)_{So\to 0} - 1\right\} = \frac{f_1}{f_{-1}} = 1\Big/\left\{\left(\frac{\vec{v}}{\bar{v}}\right)_{Si\to 0} - 1\right\}. \tag{10}$$

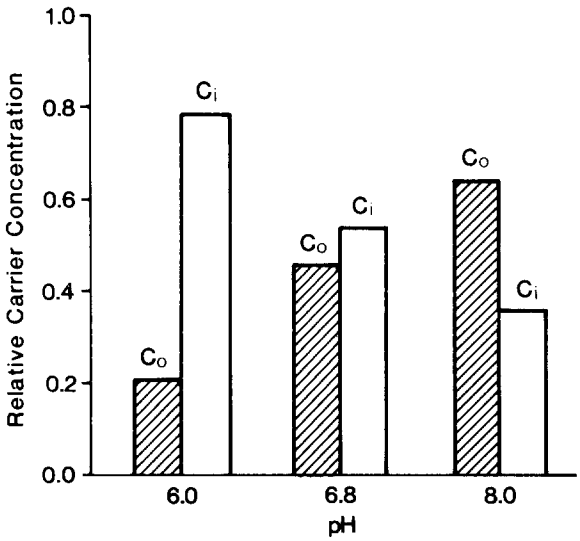

Fig. 5. Relative concentrations of the free carrier in the outward-facing and inward-facing forms (C_o and C_i, respectively), at pH 6.0, 6.8 and 8.0, in the absence of substrates or inhibitors

The data, summarized in Table 4, conform with these requirements. It may also be shown that the relative flux ratios found in the experiments at varying pH are in agreement with the predicted values from $\overline{V}_{Si}$ and $\overline{V}_{So}$, the maximum rates of exit and entry.

The effect of pH on the partition of the free carrier between the inward-facing and outward-facing forms is illustrated in the bar graph in Fig. 5.

3. Involvement of Ionizing Groups in the Translocation Mechanism

Hydrogen ions, as the above analysis has shown, increase the rate of inward movement of the free carrier $C_o \to C_i$ (governed by the rate constant f_1), and decrease the rate of outward movement, $C_i \to C_o$ (governed by f_{-1}). We may require whether any simple explanation can be attached to these findings, such as the involvement of a single ionizing group in the free carrier. That only one group need be involved is suggested by the approximately lin-

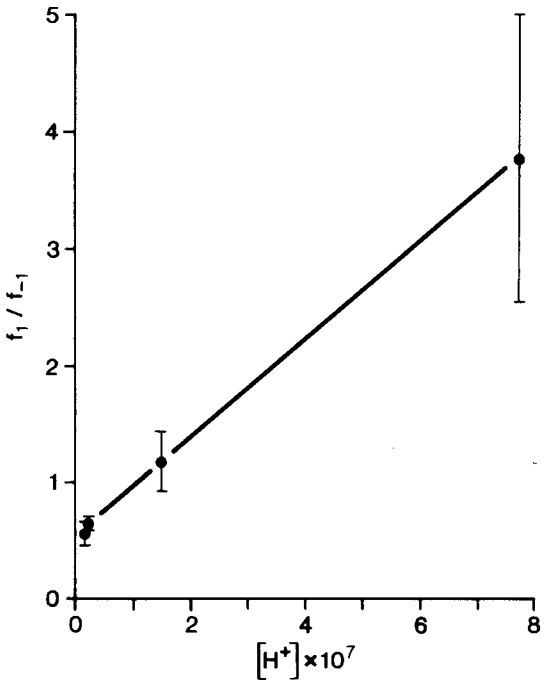

Fig. 6. Dependence of f_1/f_{-1} on the hydrogen ion concentration inside the cell. The values of f_1/f_{-1}, equal to $[C_i]/[C_o]$, were obtained from the flux ratios recorded in Table 3 (*see* Eq. 8). The internal pH was estimated from the external pH and the equilibrium distribution of chloride ions: $[H^+]_o/[H^+]_i = r_{Cl} = [Cl^-]_i/[Cl^-]_o$ (ref. 7). At external pH values of 6.0, 6.8 and 7.8, r_{Cl} was found to be 1.29, 1.09 and 0.65, respectively, in good agreement with values reported by Gunn et al. [8]

ear plot of f_1/f_{-1} versus $[H^+]$ in Fig. 6 (the relationship should be nonlinear if more than one ionizing group is involved). Though the data are not precise enough to establish the hypothesis of a single ionizing group, a further test can be applied: can trends in f_1 and f_{-1} values be accounted for individually?

The hypothesis is expressed in the reaction scheme in Fig. 7, in which a hydrogen ion can add to the inner and outer forms of the free carrier. According to this scheme the partition of the free carrier between these forms, which is equal to the ratio f_1/f_{-1}, is given by:

$$\frac{f_1}{f_{-1}} = \frac{[C_i] + [C_iH]}{[C_o] + [C_oH]} = \frac{[C_i](1 + [H^+]/K_{Hi})}{[C_o](1 + [H^+]/K_{Ho})} = \frac{f_3(1 + [H^+]/K_{Hi})}{f_{-3}(1 + [H^+]/K_{Ho})}. \quad (11)$$

It is clear from Eq. (11) that if hydrogen ions were bound with equal strength to the internal and external carrier forms ($K_{Hi} = K_{Ho}$), the partition of the carrier would not be affected by the pH of the medium. However, if K_{Hi} and K_{Ho} differ, f_1/f_{-1} will

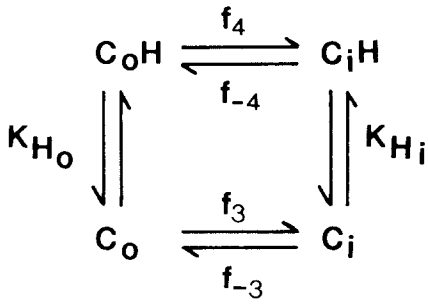

Fig. 7. Kinetic scheme in which a hydrogen ion can add to an ionizing group in the free carrier, in both the outward-facing and inward-facing forms, C_o and C_i, respectively. Addition of the proton can affect the rate of carrier reorientation (f_4 and f_{-4} as compared with f_3 and f_{-3}), as well as the partition between inner and outer forms. The scheme does not imply that the hydrogen ion is transported across the membrane, because the ionizing group may be confined to one side

be pH dependent, as the experiments require. Further, the nearly linear increase in f_1/f_{-1} with $[H^+]$ (Fig. 6) implies that under the conditions of the experiment Eq. (11) assumes a linear form, i.e., the denominator term in $[H^+]$ becomes negligible. In this case the equation reduces to:

$$\frac{f_1}{f_{-1}} = \frac{f_3}{f_{-3}}\left\{1 + \frac{[H^+]}{K_{Hi}}\right\}. \quad (12)$$

The implication is that hydrogen ions are bound much more strongly to the inner than the outer carrier form ($K_{Hi} \ll K_{Ho}$), and that the outer form is largely unprotonated in the pH range studied ($[H^+] \ll K_{Ho}$). The ionization constant of the group may be calculated from Eq. (12) and the plot in Fig. 6: $K_{Hi} \simeq 10^{-6.9}$.

In order to estimate K_{Ho} and the relative mobilities of the four forms of the free carrier (f_3, f_{-3}, f_4, and f_{-4}) it is necessary to analyze the effect of pH on f_1 and f_{-1} separately. First, we note that the rate of conversion of inner to outer carrier forms (f_{-1}) is equal to the sum of rates for the two carrier species on the inner surface, C_i and C_iH:

$$f_{-1} = \frac{f_{-3}[C_i] + f_{-4}[C_iH]}{[C_i] + [C_iH]} = \frac{f_{-3}(1 + f_{-4}[H^+]/f_{-3}K_{Hi})}{1 + [H^+]/K_{Hi}}. \quad (13)$$

Similarly, the rate of inward movement of the free carrier is given by:

$$f_1 = \frac{f_3[C_o] + f_4[C_oH]}{[C_o] + [C_oH]} = \frac{f_3(1 + f_4[H^+]/f_3K_{Ho})}{1 + [H^+]/K_{Ho}}. \quad (14)$$

The bracketed terms in the numerators of Eqs. (13) and (14) are identical, for according to the principle of microscopic reversibility,

Table 7. Experimental[a] and predicted[b] values for the partition of the free carrier (f_1/f_{-1}) and for the mobility of the inward-facing and outward-facing free carrier forms (f_{-1} and f_1, respectively), at pH 6.0, 6.8 and 8.0. All values are relative to a value of unity at pH 6.8

		pH		
		6.0	6.8	8.0
f_1/f_{-1}	Experimental	3.14 ± 1.12	1.00	0.48 ± 0.12
	Predicted	2.57	1.00	0.58
f_{-1}	Experimental	0.60 ± 0.04	1.00	1.23 ± 0.08
	Predicted	0.66	1.00	1.39
f_1	Experimental	1.88 ± 0.68	1.00	0.59 ± 0.15
	Predicted	1.71	1.00	0.81

[a] Experimental values of f_1/f_{-1} are determined from the flux ratios for exit, $(\bar{v}/v)_{Si\to 0}$ (Table 3, Eq. 8), and experimental values of f_{-1} are determined from the maximum rates of entry, $\overline{V}_{So}$ (Table 2, Eq. 1); f_1 was calculated from these values of f_1/f_{-1} and f_{-1}.
[b] Predicted values for the constants have been calculated on the basis of the reaction scheme in Fig. 7, through substitution into Eqs. (11), (13) and (16): $K_{Hi} = 10^{-6.8}$, $K_{Ho} = 10^{-5.4}$, $f_{-4}/f_{-3} = 3$.

$$\frac{f_3 K_{Ho}}{f_{-3}} = \frac{f_4 K_{Hi}}{f_{-4}}. \tag{15}$$

Substituting this relationship into Eq. (14) yields:

$$f_1 = \frac{f_3(1 + f_{-4}[H^+]/f_{-3}K_{Hi})}{1 + [H^+]/K_{Ho}}. \tag{16}$$

To solve Eqs. (13) and (16), two constants in addition to K_{Hi} must be estimated: K_{Ho} and $K_{Hi}(f_{-3}/f_{-4})$. By trial, the following values are found to give a reasonable account of the pH dependence of f_1, f_{-1} and f_1/f_{-1}, as may be seen in Table 7: $K_{Hi} = 10^{-6.8}$; $K_{Ho} = 10^{-5.4}$; $f_{-3}/f_{-4} = 3$. On the basis of these constants and an f_3/f_{-3} ratio of 0.6 (consistent with the intercept in Fig. 6), the rate constants for carrier reorientation would have the following relative values: $f_{-4} = 1$, $f_4 = 15$, $f_{-3} = 3$, $f_3 = 1.8$. The values cannot be determined with precision because of variation in the measured flux ratios with different cell samples (Table 3), but the trends are valid. We conclude that the simple mechanism in Fig. 7, involving only one ionizing group, is in accord with the results.

4. Partition of the Free Carrier in Relation to the Membrane Potential

As the pH falls from 8 to 6, the carrier partition, $[C_i]/[C_o]$, increases by a factor more than 6 (Table 7) and the chloride partition $[Cl^-]_i/[Cl^-]_o$, which is a reflection of the membrane potential, increases by a factor of 1.99 (which agrees with a factor of 1.93 reported by Gunn et al. [8]). In view of this, it must be asked whether the carrier partition could be responding, not to the pH of the solution, but to the electrical potential across the cell membrane (supposing that charged groups in the carrier move in relation to the potential gradient as the carrier undergoes reorientation).

The following argument negates this possibility. First, we calculate the number of electrical charges in the carrier that would be required to account for the observed effect. If the carrier partition is solely determined by the membrane potential (given by the Cl^- ratio), then according to the Nernst equation,

$$E_{memb} = \frac{RT}{F} \ln \frac{[Cl^-]_i}{[Cl^-]_o} = \frac{RT}{nF} \ln \frac{[C_i^{n-}]}{[C_o^{n-}]} \tag{17}$$

where the carrier site which moves from one side of the membrane to the other bears n negative charges. From Eq. (17),

$$r_{Cl} = \frac{[Cl^-]_i}{[Cl^-]_o} = \left(\frac{[C_i]}{[C_o]}\right)^{1/n} = \left(\frac{f_1}{f_{-1}}\right)^{1/n}. \tag{18}$$

Hence the carrier partition at two different membrane potentials would be related to the Cl^- ratio in the following way:

$$\left(\frac{r_{Cl_1}}{r_{Cl_2}}\right)^n = \frac{([C_i]/[C_o])_1}{([C_i]/[C_o])_2}. \tag{19}$$

Applying this relationship to the results, we find that: $(1.99)^n = 6$, and therefore $n \simeq 2.6$; i.e., the carrier should contain 2 to 3 negative charges that move across the electrical field.

The results in Table 6 show that the membrane potential does not have the expected effect. At r_{Cl} values of 1.09 and 3.21, f_1/f_{-1} (equal to $[C_i]/[C_o]$) is found experimentally to be 1.18 ± 0.24 and 0.83 ± 0.06, respectively, decreasing by a factor of roughly 0.7 (±0.21) as the chloride ratio increases by a factor of over 2.9. According to Eq. (18), f_1/f_{-1} should have increased by a factor of $(3.21/1.09)^{2.6} = 16.6$. On the other hand, if the carrier partition is solely determined by the internal pH, the observation of a small decline in f_1/f_{-1} is an expected result of the small increase in pH, 6.8 and 7.1, respectively, in the two experiments (*see* Fig. 6).

5. Possible Implications for the Carrier Mechanism

The evidence presented above shows that an ionizing group plays a role in the carrier reorientation

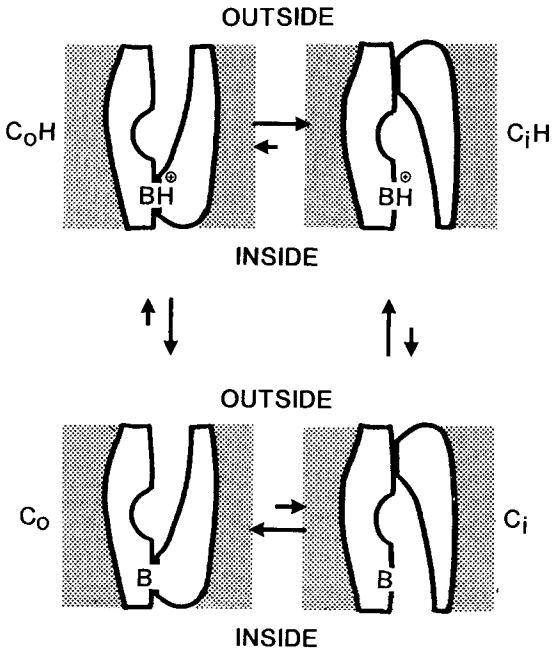

Fig. 8. Proposed involvement of an ionizing group, *B*, in a gated channel mechanism for transport. The scheme corresponds to that in Fig. 7. The ionizing group is located in the gated section of the inner channel. In the upper part of the Figure, the ionizing group is shown in the protonated, i.e. ionized form; the presence of the positive charge causes the inward-facing form of the carrier to be favored, with the charge exposed to the aqueous medium. In the lower part of the Figure, the ionizing group is in the unprotonated, i.e. uncharged, form; here the outward-facing form of the carrier is favored, with the ionizing group in the closed channel. Corresponding to these equilibria, hydrogen ions add more readily to the basic group in the inward-facing than in the outward-facing carrier

step, and we would like to propose that this group could be a component of a gating mechanism. In support of the idea we note, first, that the group appears to be outside the substrate site, a conclusion which is based on two observations: (i) the ionizing group responds to the internal but not external pH, whereas if located in the substrate site it should be exposed to the solution on both sides of the membrane; (ii) binding of a cationic substrate analog to the internal site shows no sign of being influenced by an ionization at pH 6.8, as it should with an ionizing group in or near the substrate site (R. Devés and R.M. Krupka, *unpublished data*). Nevertheless, the ionizing group and the substrate binding site are functionally associated, in that a proton is adsorbed at pH values above 6 only when the carrier is in the inward-facing form, and only from the internal solution; the same is true of the substrate site, which is accessible to substrate molecules within the cell in the inward-facing but not the outward-facing carrier.

What structure outside the substrate site, accessible to the internal but not the external solution, would be associated in this way with the substrate site in the inward-facing carrier? Clearly, a gated channel on the inner side of the membrane would have just these properties, as we have shown elsewhere [12]. It may therefore be suggested that the ionizing group is located in the wall of the inner channel, as in the model shown in Fig. 8.

We may perhaps go on to suggest that ionizing groups in the polypeptide chains lining the channels could function to alternately stabilize the open and closed states; in this mechanism they would be exposed to the aqueous medium when the channel is open but not when it is closed. There is evidence suggesting that the surfaces of the channels involved in the gating mechanism are predominantly nonpolar [12], and if so the environment of ionizing groups in this region should be less polar in the closed than in the open state. Ionization would occur most readily in polar surroundings, and consequently pK_a values would shift between the open and closed states; conversely, the ionized form would tend to stabilize the open state of the channel, and the unionized form the closed state.

If the hypothesis is correct, the ionizing group involved in the choline carrier must be assumed to be charged when protonated and neutral when unprotonated. Consequently, addition of a proton would be favored in C_i, where the environment in the open inner channel is aqueous, and disfavored in C_o, where the channel is closed and the environment nonpolar (Fig. 8). These ideas are open to further experimental tests.

We wish to thank Professor Elisa Marusic for her generosity in providing laboratory space and equipment, without which this work could not have been completed. We also thank Ms. M. Latoszek for expert technical assistance. This work was supported in part by Grant B1540-8545 from the Departmento de Desarrollo de la Investigacion, Universidad de Chile, and by a grant from the Pan-American Health Organization, to R.D.

References

1. Deuticke, B., Bayer, E., Forst, B. 1982. Discrimination of three parallel pathways of lactate transport in the human erythrocyte membrane by inhibitors and kinetic properties. *Biochim. Biophys. Acta* **684**:96–110
2. Devés, R., Krupka, R.M. 1979. A general kinetic analysis of transport. Tests of the carrier model based on predicted relations among experimental parameters. *Biochim. Biophys. Acta* **556**:533–547
3. Devés, R., Krupka, R.M. 1979. The binding and translocation steps in transport as related to substrate structure. A study of the choline carrier of erythrocytes. *Biochim. Biophys. Acta* **557**:469–485

4. Devés, R., Krupka, R.M. 1981. Evidence for a two-state mobile carrier mechanism in erythrocyte choline transport: Effects of substrate analogs on inactivation of the carrier by N-ethylmaleimide. *J. Membrane Biol.* **61**:21–30
5. Devés, R., Krupka, R.M. 1983. Apparent noncompetitive inhibition of choline transport in erythrocytes by inhibitors bound at the substrate site. *J. Membrane Biol.* **74**:183–189
6. Edwards, P.A. 1973. Evidence for the carrier model of transport from inhibition by N-ethylmaleimide of choline transport across the human red cell membrane. *Biochim. Biophys. Acta* **311**:123–140
7. Freedman, J.C., Hoffman, J.F. 1979. The relation between dicarbocyanine dye fluorescence and the membrane potential of human red blood cells set at varying Donnan equilibria. *J. Gen. Physiol.* **74**:187–212
8. Gunn, R.B., Dalmark, M., Tosteson, D.C., Wieth, J.O. 1973. Characteristics of chloride transport in human red blood cells. *J. Gen. Physiol.* **61**:185–206
9. Krupka, R.M., Devés, R. 1980. The choline transport system of erythrocytes. Distribution of the free carrier in the membrane. *Biochim. Biophys. Acta* **600**:228–232
10. Krupka, R.M., Devés, R. 1981. An experimental test for cyclic versus linear transport models. *J. Biol. Chem.* **256**:5410–5416
11. Krupka, R.M., Devés, R. 1983. Kinetics of inhibition of transport systems. *Int. Rev. Cytol.* **84**:303–352
12. Krupka, R.M., Devés, R. 1986. Looking for probes of gated channels: Studies of the inhibition of glucose and choline transport in erythrocytes. *Can. J. Biochem. Cell Biol.* (*in press*)
13. Martin, K. 1968. Concentrative accumulation of choline by human erythrocytes. *J. Gen. Physiol.* **51**:497–516
14. Martin, K. 1971. Some properties of an SH group essential for choline transport in human erythrocytes. *J. Physiol.* (*London*) **213**:647–664
15. Wharton, C.W. 1983. Some recent advances in enzyme kinetics. *Biochem. Soc. Trans.* **11**:817–825

Received 13 February 1986; revised 13 May 1986